

## Introduction

Marchenko imaging is a novel imaging technique that is capable to retrieve images from single-sided reflection measurements free of artefacts related to internal multiples (e.g. Behura et al., 2014; Brogini et al., 2012). An essential ingredient of Marchenko imaging is the so-called focusing function which can be retrieved from reflection data and a background model. Initially, the focusing function was defined such that it focuses inside the medium of interest as a point in time and in space (e.g. Wapenaar et al., 2014). The focusing property is used to retrieve the up- and downgoing Green's functions associated to a virtual point source or receiver inside the medium. Subsequently, the retrieved Green's functions are used to compute an image. Meles et al. (2017) introduced a new focusing function that focuses as a plane wave inside the medium. The new focusing function allows to retrieve medium responses associated to virtual plane wave sources or receivers inside the medium. Hence, imaging based on areal-sources as suggested by Rietveld et al. (1992) becomes possible including the benefits of the Marchenko method. In the following we compare Marchenko imaging using point and plane wave focusing.

## Point focusing

In this section we review conventional Marchenko imaging which uses point focusing. We consider a lossless medium that can be acoustic or elastic. Assuming that the medium has infinite lateral extent and is bounded at the top by a reflection-free boundary  $\partial\mathbb{D}_0$  one can derive the following two expressions from the reciprocity theorems of the convolution- and correlation-type (for a detailed derivation we refer to e.g. Wapenaar et al., 2014),

$$\hat{\mathbf{f}}_1^-(\mathbf{x}', \mathbf{x}_f, \omega) + \{\hat{\mathbf{g}}^-(\mathbf{x}_f, \mathbf{x}', \omega)\}^T = \int_{\partial\mathbb{D}_0} \hat{\mathbf{R}}(\mathbf{x}', \mathbf{x}, \omega) \hat{\mathbf{f}}_1^+(\mathbf{x}, \mathbf{x}_f, \omega) d^2\mathbf{x}_H, \quad (1)$$

$$\hat{\mathbf{f}}_1^+(\mathbf{x}', \mathbf{x}_f, \omega) - \{\hat{\mathbf{g}}^+(\mathbf{x}_f, \mathbf{x}', \omega)\}^\dagger = \int_{\partial\mathbb{D}_0} \hat{\mathbf{R}}^*(\mathbf{x}', \mathbf{x}, \omega) \hat{\mathbf{f}}_1^-(\mathbf{x}, \mathbf{x}_f, \omega) d^2\mathbf{x}_H. \quad (2)$$

Here, we use one-way power-flux normalised wavefield potentials: the Green's function  $\hat{\mathbf{g}}^\pm$ , the focusing function  $\hat{\mathbf{f}}_1^\pm$  and the reflection response  $\hat{\mathbf{R}}$ . In addition, we neglect evanescent waves. The superscripts "+" and "-" describe down- and upgoing waves, respectively. We denote complex conjugation by a "\*", transposition by a "T" and complex-conjugate transpose by a "†". For all wavefield potentials the first coordinate refers to the receiver position  $\mathbf{x} = (x_1, x_2, x_3)^T$ , the second coordinate refers to the source (or focusing) position and the third coordinate refers to the temporal frequency  $\omega$ . The subscript "H" denotes the horizontal coordinates, i.e.  $\mathbf{x}_H = (x_1, x_2)^T$ . Further, we use hats (" ^ ") for quantities in the frequency domain. All equations in this abstract are valid for acoustic as well as elastodynamic waves. Wavefield potentials are scalars for the acoustic case and  $3 \times 3$  matrices for the elastodynamic case. For example, the elastodynamic downgoing focusing function can be written as,

$$\hat{\mathbf{f}}_1^+(\mathbf{x}', \mathbf{x}_f, \omega) = \begin{pmatrix} (\hat{f}_1^+)_{\Phi, \Phi} & (\hat{f}_1^+)_{\Phi, \Psi} & (\hat{f}_1^+)_{\Phi, \Upsilon} \\ (\hat{f}_1^+)_{\Psi, \Phi} & (\hat{f}_1^+)_{\Psi, \Psi} & (\hat{f}_1^+)_{\Psi, \Upsilon} \\ (\hat{f}_1^+)_{\Upsilon, \Phi} & (\hat{f}_1^+)_{\Upsilon, \Psi} & (\hat{f}_1^+)_{\Upsilon, \Upsilon} \end{pmatrix} (\mathbf{x}', \mathbf{x}_f, \omega), \quad (3)$$

where the subscripts  $\Phi$ ,  $\Psi$  and  $\Upsilon$  refer to P-, S1- and S2-wavefield potentials, respectively. The first and second subscript describe the wavefield potential at the receiver position  $\mathbf{x}'$  and at the focusing (or source) position  $\mathbf{x}_f$ , respectively. The focusing function  $\hat{\mathbf{f}}_1$  is a wavefield that is injected into the medium at the upper boundary  $\partial\mathbb{D}_0$  and focuses at time zero at the focusing position  $\mathbf{x}_f$ . In the space-time domain, the focusing property can be formulated as,

$$\mathbf{f}_1^+(\mathbf{x}', \mathbf{x}_f, t) \Big|_{x'_3=x_{3,f}} = \delta(t) \delta(\mathbf{x}'_H - \mathbf{x}_{H,f}) \mathbf{I}, \quad (4)$$

where  $\mathbf{I}$  is an identity matrix of appropriate size (a scalar for the acoustic case). We write the focusing property (Eq. 4) in the space-time domain to emphasise that it describes a focus in space and in time. In many imaging applications the medium of interest is only accessible from a single boundary. Hence, in Eqs. 1-2 only the reflection response  $\hat{\mathbf{R}}$  is known such that the system of Eqs. 1-2 is underdetermined. However, several publications (e.g. Van der Neut et al., 2015) have shown that focusing and Green's

functions can be separated in the time domain. After applying a separation operator  $\theta$ , Eqs. 1-2 become the coupled Marchenko equations,

$$\hat{\mathbf{f}}_1^-(\mathbf{x}', \mathbf{x}_f, \omega) = \theta \circ \int_{\partial\mathbb{D}_0} \hat{\mathbf{R}}(\mathbf{x}', \mathbf{x}, \omega) (\hat{\mathbf{f}}_{1,0}^+ + \hat{\mathbf{f}}_{1,m}^+) (\mathbf{x}, \mathbf{x}_f, \omega) d^2\mathbf{x}_H, \quad (5)$$

$$\hat{\mathbf{f}}_{1,m}^+(\mathbf{x}', \mathbf{x}_f, \omega) = \theta \circ \int_{\partial\mathbb{D}_0} \hat{\mathbf{R}}^*(\mathbf{x}', \mathbf{x}, \omega) \hat{\mathbf{f}}_1^-(\mathbf{x}, \mathbf{x}_f, \omega) d^2\mathbf{x}_H, \quad (6)$$

which can be solved for  $\hat{\mathbf{f}}_{1,m}^+$  and  $\hat{\mathbf{f}}_1^-$ , assuming  $\hat{\mathbf{f}}_{1,0}^+$  is known. In Eqs. 5-6 we separated the downgoing focusing function into a direct (or in the elastodynamic case forward-scattered) part  $\hat{\mathbf{f}}_{1,0}^+$  and a coda  $\hat{\mathbf{f}}_{1,m}^+$ . The circle "o" denotes a Hadamard product. To obtain the desired Green's functions  $\hat{\mathbf{g}}^\pm$  we evaluate Eqs. 1-2 using the retrieved focusing functions  $\hat{\mathbf{f}}_1^\pm$ . The resulting Green's functions are associated with virtual recordings inside the medium and can be used for imaging. Here, we use redatumed reflectivity  $\hat{\mathbf{r}}$  and a standard migration imaging condition  $\mathbf{i}_c$  in the frequency domain,

$$\hat{\mathbf{r}}(\mathbf{x}_f, \omega) = \int_{\partial\mathbb{D}_0} \hat{\mathbf{g}}^-(\mathbf{x}_f, \mathbf{x}', \omega) \{\hat{\mathbf{g}}_d^+(\mathbf{x}_f, \mathbf{x}', \omega)\}^\dagger d^2\mathbf{x}'_H, \quad (7)$$

$$\mathbf{i}_c(\mathbf{x}_f) = \int \hat{\mathbf{r}}(\mathbf{x}_f, \omega) d\omega, \quad (8)$$

where  $\hat{\mathbf{g}}_d^+(\mathbf{x}_f, \mathbf{x}', \omega)$  is a direct Green's function in a background model. Since the Green's function  $\hat{\mathbf{g}}^-$  in Eq. 7 describes all orders of scattering correctly the image  $\mathbf{i}_c$  is free of artefacts related to internal multiples. Note that Eqs. 7-8 imply that the Green's function  $\hat{\mathbf{g}}^-$  must be determined for each imaging point  $\mathbf{x}_f$ , therefore, we refer to this imaging method as Marchenko point imaging.

Next, we show a numerical example of Marchenko point imaging. To this end, we model the reflection response of a 2D acoustic model (see Fig. 1a). We use the background model of Fig. 1b to retrieve the Green's functions  $\hat{\mathbf{g}}^-$  via the Marchenko method and compute an image according to Eqs. 7-8. We repeat this process for each imaging point. The resulting image is displayed in Fig. 2a. The image is close to the true model. In particular, it is free of artefacts caused by internal multiples.

### Plane wave focusing

The focusing condition in Eq. 4 states that the focusing function  $\hat{\mathbf{f}}_1^\pm$  focuses as a point in the space-time domain. Therefore, we will refer to  $\hat{\mathbf{f}}_1^\pm$  as point focusing function. Following recent insights on focusing conditions (Meles et al., 2017) we suggest to define a plane wave focusing function  $\hat{\mathbf{F}}_1^\pm$  that focuses as a plane wave in the space-time domain,

$$\mathbf{F}_1^+(\mathbf{x}', \mathbf{p}_H, x_{3,f}, t) \Big|_{x'_3=x_{3,f}} = \delta(t - \mathbf{p}_H \cdot \mathbf{x}'_H) \mathbf{I}, \quad (9)$$

where the horizontal ray-parameter is denoted by  $\mathbf{p}_H$ . The plane wave focusing condition in Eq. 9 can be obtained by convolving the point focusing condition in Eq. 4 with  $\delta(t - \mathbf{p}_H \cdot \mathbf{x}_{H,f})$  in the time domain and integrating the result along  $\mathbf{x}_{H,f}$ . Hence, to obtain the plane wave focusing function  $\hat{\mathbf{F}}_1^\pm(\mathbf{x}', \mathbf{p}_H, x_{3,f}, \omega)$  in the space-frequency domain we multiply the point focusing function  $\hat{\mathbf{f}}_1^\pm(\mathbf{x}', \mathbf{x}_{H,f}, x_{3,f}, \omega)$  by  $e^{j\omega\mathbf{p}_H \cdot \mathbf{x}_{H,f}}$  and integrate the result along  $\mathbf{x}_{H,f}$ ,

$$\hat{\mathbf{F}}_1^\pm(\mathbf{x}', \mathbf{p}_H, x_{3,f}, \omega) = \int_{\partial\mathbb{D}_f} \hat{\mathbf{f}}_1^\pm(\mathbf{x}', \mathbf{x}_{H,f}, x_{3,f}, \omega) e^{j\omega\mathbf{p}_H \cdot \mathbf{x}_{H,f}} d^2\mathbf{x}_{H,f}. \quad (10)$$

Here, the boundary  $\partial\mathbb{D}_f$  refers to the depth level  $x_3 = x_{3,f}$ . Analogous to Eq. 10 we define a plane wave response,

$$\hat{\mathbf{G}}^\pm(-\mathbf{p}_H, x_{3,f}, \mathbf{x}', \omega) = \int_{\partial\mathbb{D}_f} \hat{\mathbf{g}}^\pm(\mathbf{x}_{H,f}, x_{3,f}, \mathbf{x}', \omega) e^{j\omega\mathbf{p}_H \cdot \mathbf{x}_{H,f}} d^2\mathbf{x}_{H,f}. \quad (11)$$

Subsequently, we multiply Eqs. 1-2 by  $e^{j\omega\mathbf{p}_H \cdot \mathbf{x}_{H,f}}$ , integrate the results over the surface  $\partial\mathbb{D}_f$ , use Eqs. 10-11 and obtain,

$$\hat{\mathbf{F}}_1^-(\mathbf{x}', \mathbf{p}_H, x_{3,f}, \omega) + \{\hat{\mathbf{G}}^-(\mathbf{p}_H, x_{3,f}, \mathbf{x}', \omega)\}^T = \int_{\partial\mathbb{D}_0} \hat{\mathbf{R}}(\mathbf{x}', \mathbf{x}, \omega) \hat{\mathbf{F}}_1^+(\mathbf{x}, \mathbf{p}_H, x_{3,f}, \omega) d^2\mathbf{x}, \quad (12)$$

$$\hat{\mathbf{F}}_1^+(\mathbf{x}', \mathbf{p}_H, x_{3,f}, \omega) - \{\hat{\mathbf{G}}^+(\mathbf{p}_H, x_{3,f}, \mathbf{x}', \omega)\}^\dagger = \int_{\partial\mathbb{D}_0} \hat{\mathbf{R}}^*(\mathbf{x}', \mathbf{x}, \omega) \hat{\mathbf{F}}_1^-(\mathbf{x}, \mathbf{p}_H, x_{3,f}, \omega) d^2\mathbf{x}. \quad (13)$$

The expressions in Eqs. 12-13 are again an underdetermined system of equations. However, it has been observed that the plane wave focusing functions  $\hat{\mathbf{F}}_1^\pm(\mathbf{x}', \mathbf{p}_H, x_{3,f}, \omega)$  can be separated from the plane wave responses  $\hat{\mathbf{G}}^\pm(-\mathbf{p}_H, x_{3,f}, \mathbf{x}', \omega)$  in the space-time domain (Meles et al., 2017). Thus, analogous to the point Marchenko method after applying a separation operator Eqs. 12-13 become the coupled Marchenko equations which can be solved. In order to compute an image from the resulting plane wave responses  $\hat{\mathbf{G}}^\pm(-\mathbf{p}_H, x_{3,f}, \mathbf{x}', \omega)$  we multiply the redatumed reflectivity (Eq. 7) as well as the standard migration imaging condition (Eq. 8) by  $e^{j\omega \mathbf{p}_H \cdot \mathbf{x}_{H,f}}$ , integrate the results along  $\mathbf{x}_{H,f}$  and find,

$$\hat{\mathbf{R}}(-\mathbf{p}_H, \mathbf{x}_{H,f}, x_{3,f}, \omega) = \int_{\partial \mathbb{D}_0} \hat{\mathbf{G}}^(-\mathbf{p}_H, x_{3,f}, \mathbf{x}', \omega) \{ \hat{\mathbf{g}}_d^+(\mathbf{x}_f, \mathbf{x}', \omega) \}^\dagger d^2 \mathbf{x}'_H, \quad (14)$$

$$\mathbf{I}_c(\mathbf{p}_H, \mathbf{x}_{H,f}, x_{3,f}) = \int \hat{\mathbf{R}}(-\mathbf{p}_H, \mathbf{x}_{H,f}, x_{3,f}, \omega) e^{j\omega \mathbf{p}_H \cdot \mathbf{x}_{H,f}} d\omega. \quad (15)$$

The plane wave imaging condition (Eq. 15) only takes into account a single ray-parameter, i.e. it is illuminating the image point  $\mathbf{x}_f$  from a single angle. In contrast, the point imaging condition (Eq. 8) uses implicitly all ray-parameters, ergo, it is illuminating the image point  $\mathbf{x}_f$  from a range of angles. The benefit of the plane wave imaging condition is that it only requires one plane wave response  $\hat{\mathbf{G}}^-$  per depth level  $\partial \mathbb{D}_f$  whereas the point imaging condition requires one Green's function  $\hat{\mathbf{g}}^-$  for each image point on a depth level  $\partial \mathbb{D}_f$ . In other words if there are  $N$  image points per depth level, plane wave imaging reduces the computational costs by a factor of  $N$  compared to point imaging.

To illustrate the differences between point and plane wave imaging we retrieve the plane wave responses  $\hat{\mathbf{G}}^-$  using the reflection responses of the model in Fig. 1a as well as the smooth background model in Fig. 1b. In this example we consider the plane wave component  $p_1 = 0 \text{ s m}^{-1}$ . The resulting image is shown in Fig. 2b. Comparison to a migration image using standard extrapolation of virtual plane waves (see Fig. 2c) demonstrates that the plane wave Marchenko image does not suffer from artefacts due to internal multiples. Despite using a single plane wave component the plane wave Marchenko image is nearly as good as the point image which uses all plane wave components. Yet, a close look at the image in Fig. 2b-c reveals that the plane wave images lack a reflector at about  $x_3 = 1100 \text{ m}$ . In fact, the reflection coefficient of the missing reflector for a ray-parameter  $p_1 = 0 \text{ s m}^{-1}$  is about 100 times smaller than the strongest reflection coefficient of model. This explains why plane wave imaging can hardly detect the missing reflector.

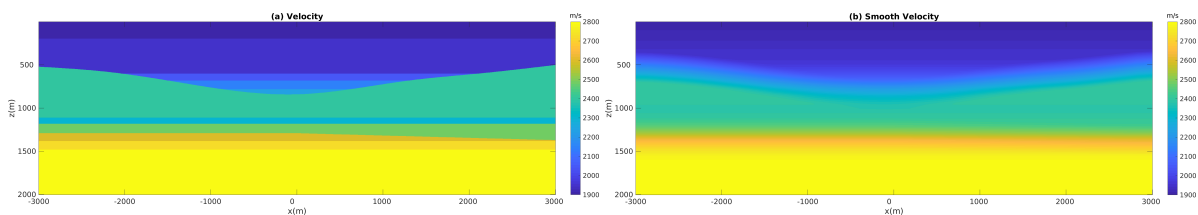


Figure 1: (a) True and (b) smooth velocity model. The true and smooth density model have a similar spatial variation as the velocity model, however, they are not displayed.

## Discussion and conclusions

We demonstrated two imaging strategies using point and plane wave focusing conditions. Both approaches use medium responses that are retrieved from reflection data and a background model via the Marchenko method. In consequence, both strategies take into account all orders of scattering correctly, resulting in images free of artefacts due to internal multiples. The plane wave imaging condition, compared to point Marchenko imaging, reduces the computational costs significantly but provides less illumination of each image point. Plane wave Marchenko imaging raises the opportunity to apply imaging for a limited number of plane wave components to meet a case dependent illumination versus cost balance.

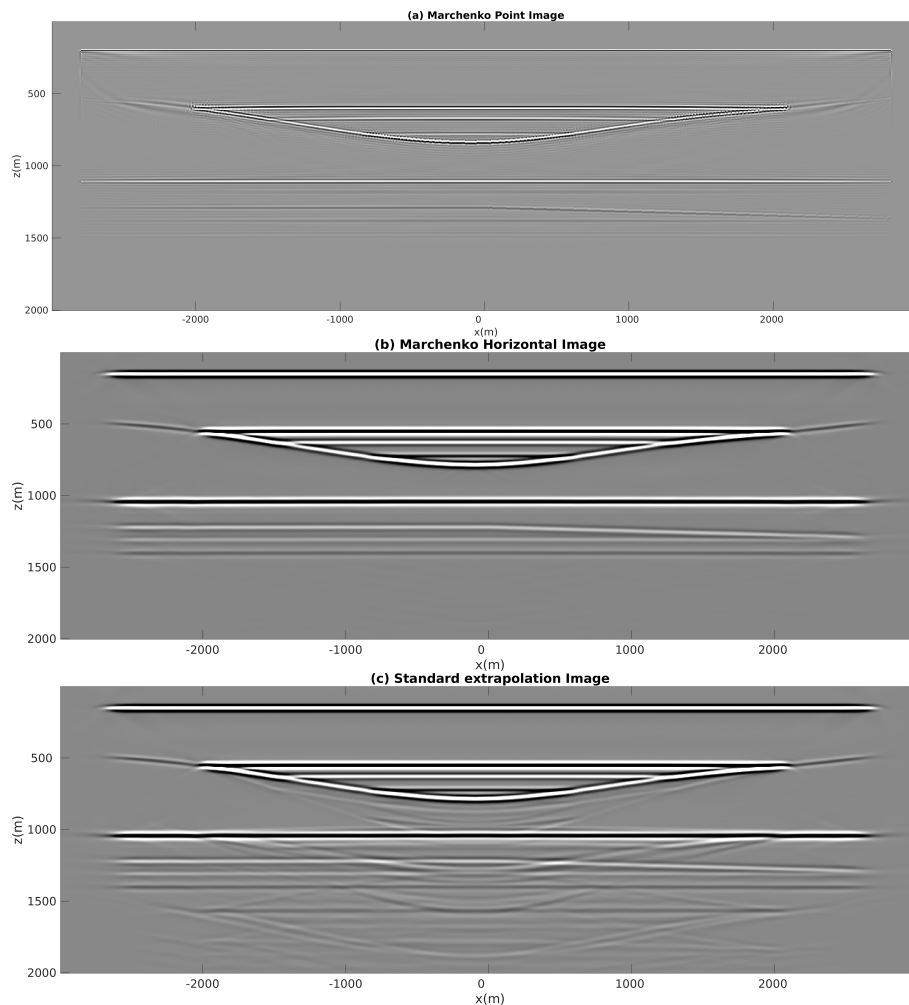


Figure 2: (a) Migration result using imaging condition of Eq. 8 and virtual point responses  $\hat{\mathbf{g}}^-$  retrieved via the Marchenko method. (b) Migration result using imaging condition of Eq. 15 and virtual plane wave responses  $\hat{\mathbf{G}}^-$  retrieved via the Marchenko method. (c) Migration result using virtual plane wave responses  $\hat{\mathbf{G}}^-$  retrieved via standard wavefield extrapolation. Images (b) and (c) correspond to a plane wave defined by  $p_1 = 0 \text{ s m}^{-1}$ .

## References

- Behura, J., Wapenaar, K., & Snieder, R., 2014. Autofocus imaging: Image reconstruction based on inverse scattering theory, *Geophysics*, **79**(3), A19–A26.
- Broggini, F., Snieder, R., & Wapenaar, K., 2012. Focusing inside an unknown medium using reflection data with internal multiples: Numerical examples for a laterally-varying velocity model, spatially-extended virtual source, and inaccurate direct arrivals, *SEG Technical Program Expanded Abstracts 2012*, pages 1-5.
- Meles, G. A., Wapenaar, K., & Thorbecke, J., 2017. Virtual plane-wave imaging via Marchenko redatuming, *arXiv preprint arXiv:1711.11424 A*.
- Rietveld, W., Berkhout, A., & Wapenaar, C., 1992. Optimum seismic illumination of hydrocarbon reservoirs, *Geophysics*, **57**(10), 1334–1345.
- Van der Neut, J., Vasconcelos, I., & Wapenaar, K., 2015. On Green's function retrieval by iterative substitution of the coupled Marchenko equations, *Geophysical Journal International*, **203**(2), 792–813.
- Wapenaar, K., Thorbecke, J., Van der Neut, J., Broggin, F., Slob, E., & Snieder, R., 2014. Green's function retrieval from reflection data, in absence of a receiver at the virtual source position, *Acoustical Society of America*, **135**(5), 2847-2861.